






Secondary flow in contour currents controls the formation of moat-drift contourite systems

Henriette Wilckens ^{1,2}✉, Joris T. Eggenhuisen ³, Pelle H. Adema ³, F. Javier Hernández-Molina^{4,5}, Ricardo Silva Jacinto ⁶ & Elda Miramontes ^{1,2}

Ocean currents control seafloor morphology and the transport of sediments, organic carbon, nutrients, and pollutants in deep-water environments. A better connection between sedimentary deposits formed by bottom currents (contourites) and hydrodynamics is necessary to improve reconstructions of paleocurrent and sediment transport pathways. Here we use physical modeling in a three-dimensional flume tank to analyse the morphology and hydrodynamics of a self-emerging contourite system. The sedimentary features that developed on a flat surface parallel to a slope are an elongated depression (moat) and an associated sediment accumulation (drift). The moat-drift system can only form in the presence of a secondary flow near the seafloor that transports sediment from the slope toward the drift. The secondary flow increases with higher speeds and steeper slopes, leading to steeper adjacent drifts. This study shows how bottom currents shape the morphology of the moat-drift system and highlights their potential to estimate paleo-ocean current strength.

¹Faculty of Geosciences, University of Bremen, Bremen, Germany. ²MARUM - Center for Marine Environmental Sciences, University of Bremen, Bremen, Germany. ³Faculty of Geosciences, Utrecht University, P.O. Box 80021TA Utrecht, Netherlands. ⁴Department of Earth Sciences, Royal Holloway University of London, Egham, Surrey, UK. ⁵Marine Geosciences Division, CSIC & UGR, IACT, Armilla Granada, Spain. ⁶UMR 6538 GEO-OCEAN, Ifremer, Univ Brest, CNRS, Univ. Bretagne-Sud, Plouzané, France. ✉email: cwilcken@uni-bremen.de

Oceanic currents play an important role in climate and ecosystems and can strongly impact sedimentation and seafloor morphology in deepwater environments. These currents transport sediment, microplastics, and organic matter^{1,2}. Establishing a conceptual model that integrates the current dynamics and the morphology of a contourite system can help to understand the sediment transport pathways and how that affects ecosystems. As ocean currents will be modified under the present climate change³ predicting how these currents evolve under different climatic situations could be improved by understanding how the ocean system changed in the past. Paleoreconstructions of ocean currents can be performed by analysing contourites, which are the sediment accumulations that have been substantially affected by currents flowing near the seafloor (i.e., bottom currents)⁴. Paleocurrent information can be obtained from grain size analyses of sediment cores and of the internal sediment architecture using seismic data^{5–9}. However, our poor understanding of linking hydrodynamic processes with contourite features limits the integration of seismic data for quantitative paleoceanographic reconstructions¹⁰. Thus, current speed reconstructions are mostly based on grain size of samples from sediment cores^{8,9,11}, or only provide rough estimates depending on the observed bedforms¹². Sediment cores only provide very local information and spacing between cores often exceeds the size of architectural elements within a contourite system. Combining core data with regional data sets, which can be obtained from bathymetric and seismic data, improves paleoceanographic interpretations¹³. Furthermore, velocity measurements from bottom currents in the deep sea are very scarce¹⁴, due to the depth limitations of vessel-mounted acoustic currentmeters (commonly upper ~1000 m of the ocean)^{15,16} and the logistics and economic costs of maintaining moorings in deep-water environments. In contrast, multibeam bathymetric data is nowadays more frequently collected in the deep sea. Thus, a stronger understanding of the link between bathymetry and ocean currents would help to understand today's current dynamics and possibly help to suggest where focused measurements are needed to reveal the spatial variability of bottom currents.

In this study, we analyze the processes that control the development of a contourite depositional system which consists of an elongated depression parallel to a submarine slope, called a 'moat', and an associated sedimentary deposit named an 'elongated and separated mounded drift' that forms seaward and parallel to the moat^{4,10}. They are typically found at slope breaks, which can be the foot of the continental slope (slope-basin floor transition), the foot of a seamount, a landslide scar, a fault, a cold-water coral mound, a contourite terrace, or any other feature creating a strong local perturbation on the continental slope^{1,4,10,17}. These systems show high variability in terms of width and depth as well as seismic stratigraphy¹⁷. Moats can be driven by sediment erosion (Fig. 1a), or they can be more constructional (Fig. 1b) due to lower sedimentation inside the moat compared to the drift alongside the moat¹⁷. Moat-drift systems provide a clear indication of the dominant bottom current direction, which is useful for reconstructing bottom currents^{5,18,19}. However, the characteristics of the current, in terms of strength and local hydrodynamics, cannot currently be deduced from the moat and drift characteristics^{10,15,20,21}. Moats have been interpreted to have formed at the location of the velocity core of the current (Fig. 1c)^{15,22,23}. Several authors have hypothesized a helicoidal flow structure over the moat, but the suggested spin direction differs between authors^{4,21,24}. The helicoidal concept has not been supported by measurements or theory yet, and it remains unclear whether such a structure is a necessary condition for the emergence of moats, or whether it forms as a result of hydrodynamic interaction between existing moats and active contour currents. To date, vessel-mounted acoustic Doppler current profiler data has not been

able to confirm the existence of a helicoidal flow over moats. Yet, this reality could simply be due to the poor resolution of the data near the seafloor and the limited amount of data collected over moats in the first place¹⁵.

This study presents the first analysis of a contourite depositional system developed in a 3D flume tank (EUROTANK) at Utrecht University (Fig. 2). We focus on a contourite depositional system that consists of a moat and a separated mounded drift. A circulation system generates a current flowing parallel to the slope of the tank, as an analog for a contour current flowing parallel to a continental margin. For the analysis of the bathymetric evolution of the contourite system, we calculate the average along-slope elevation of a 70 cm wide swath in the middle of the tank (Fig. 2) and plot the data as one cross-section (Fig. 3). This procedure averages out the bathymetric perturbations of unscaled ripples (Fig. 2b).

The analyses of the contourite depositional system that develops in the flume tank test the following hypotheses: (1) moats and drifts migrate upslope with higher sediment availability; (2) the morphology of moats and drifts depends on current speed; and (3) there is a secondary across-slope flow in the moat-drift system that depends on the along-slope velocity and the steepness of the continental slope.

Results

Morphological evolution. All six experiments start with the same base morphology, comprising a terrace and a slope (with a slope gradient of 18° or 26°). In all experiments, we distinguish between two phases. In the sediment input phase (first phase), 80 dm³ of sediment is added via the sediment feeder. In the reworking phase (second phase), the sediment is reworked by the flow while no extra sediment is added to the flume tank.

Experiment 1: Sediment input affects moat-drift migration. Experiment 1 shows how the morphology evolves in response to changes in sediment input (Fig. 3). In the first phase, sediment is added to the tank and transported to the study area by an 18 cm/s current. This leads to an elongated depression parallel to the 18° slope (a moat) and an adjacent basinward elongated mounded drift (Fig. 3a). The moat migrates downslope in the second phase of the experiment, during which no sediment is supplied (Fig. 3a). In the third phase, sediment is supplied again, and the moat migrates upslope due to the formation of a sigmoidal deposit (Fig. 3b).

Experiments 2–6: Slope angle and current velocity affects moat-drift morphology. In experiments 2–4, the moat-drift system develops at an 18° slope with different current velocities. Three velocities are tested with the same slope-terrace setup. The experiments consist of one sediment input phase and a subsequent reworking phase. After a moat-drift system is formed, we measure the width between the drift crest and the slope, relief (depth between moat trough and drift crest), and drift angle (slope angle of the drift on the side of the moat) (Table 1). In experiment 2, with a low speed of 11 cm/s, sediment drapes the slope and terrace, but no moat develops even after an extra 9 h of sediment reworking (Fig. 4a). In experiment 3, with a medium speed of 16 cm/s, a small moat develops with a drift angle of 8° (Fig. 4b). A faster current speed of 18 cm/s in experiment 4 creates a larger moat with a higher drift angle of 11° (Fig. 4c), compared to experiments 2 and 3, which have lower current speeds.

Experiments 5 and 6 are similar to experiments 2–3 with input and reworking phases but the slope increased to 26°. Here, two different current speeds are tested (Table 1). In experiment 5,

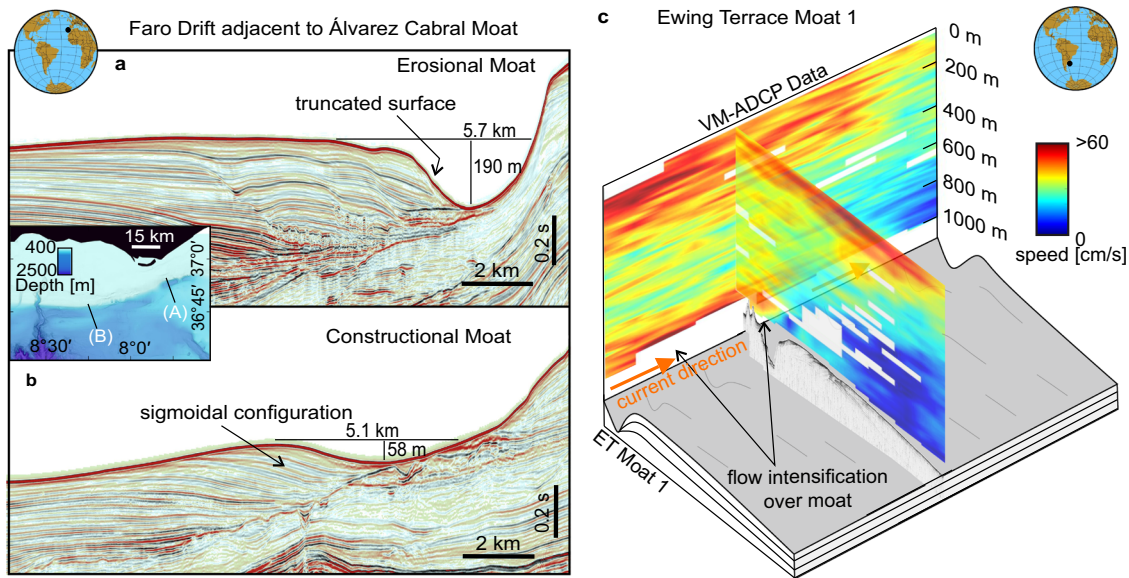


Fig. 1 Moat-drift systems show a large variety in morphology and seismic stratigraphy. The figure shows a seismic cross-section of the Álvaro Cabral Moat in the Gulf of Cadiz located (a) upstream and (b) downstream of the bottom current. (c) Vessel-mounted acoustic Doppler current profiler (VM-ADCP) data and sub-bottom profiler at the Argentine continental margin show a flow intensification over the moat (modified from¹⁵).

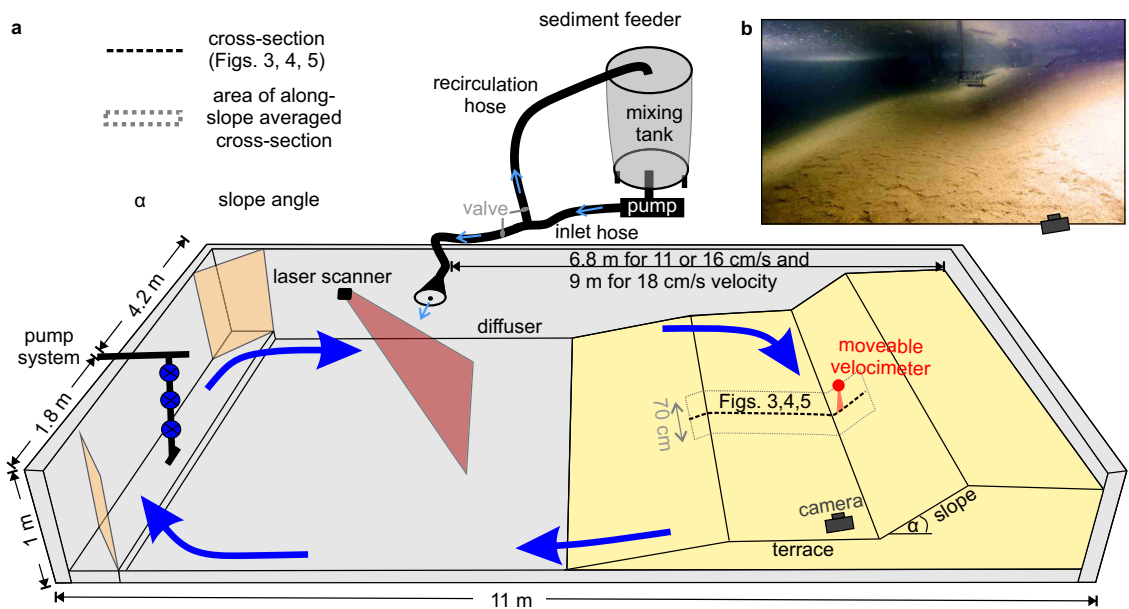


Fig. 2 Experimental setup. (a) Schematic drawing of the experimental setup (b) Underwater photo of the flume tank floor and the velocimeter. Modified from⁵¹.

with a low current speed of 11 cm/s, a small moat with a drift angle of 4° develops (Fig. 4d). In experiment 6, the drift angle increases to 15° when running the experiment with a stronger current speed of 16 cm/s (Fig. 4e).

Current velocity measurements. Current velocity is measured at the base of the slope at the lowest 10 cm above the bed (Fig. 4a–e). All velocity measurements presented in Fig. 4 are carried out before the moat-drift system was established. For all experiments, the velocity is stronger along-slope. For the low current speed setting with the 18° slope, there is a small secondary flow towards the slope. For the other settings, with a stronger along-slope velocity or a steeper slope, the current direction depends on the distance above the bed. For the secondary flow (vertical plan

cross-slope), the velocity at ~5 cm above the bed is directed towards the slope but in the lowest ~5 cm above the bed, the bottom current is flowing away from the slope (Fig. 4b–e).

Across-slope velocity measurements, carried out during the first hour of the experiment with the fastest current setting and a slope angle of 18°, show that the along-slope velocity is higher near the slope and decreases on the terrace (Fig. 5a). At the beginning of the experiments in the first 5 cm above the bed on the lower slope, the across-slope velocity is directed away from the slope and the current is flowing over the terrace towards the basin (Fig. 5b). At approximately 5–10 cm above the bed, the across-slope velocity is directed towards the slope (Fig. 5b). Furthermore, at the lower slope, the vertical velocity is directed downwards and at the basinward side of the terrace, it is directed

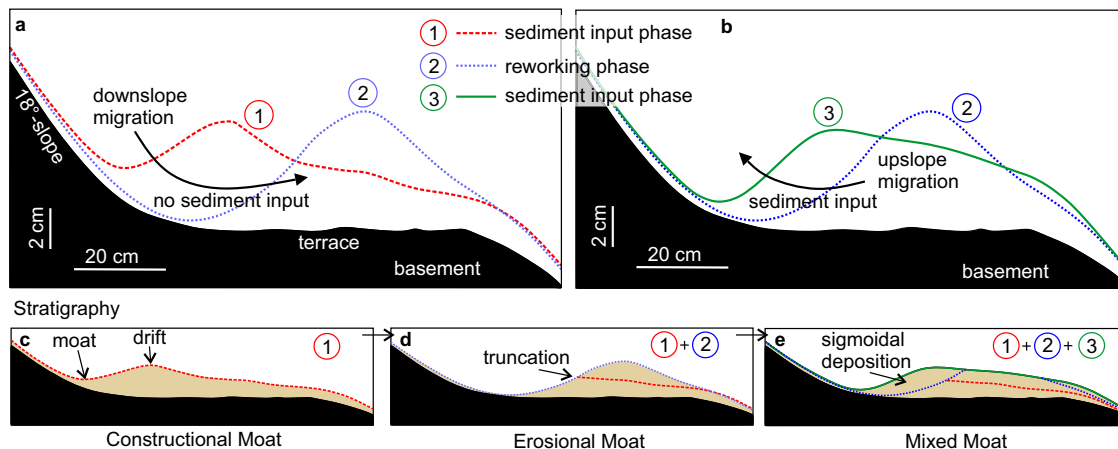


Fig. 3 Comparison of moat-drift migration without and with sediment input (Experiment 1). Measured cross-sections from moat-drift systems show that (a) a moat migrates downslope when no sediment is available and (b) a moat can migrate upslope when sediment is supplied. (c) The moat self-emerges after the sediment input phase. (d) Stratigraphy of a moat with no sediment input. (e) Stratigraphy of a moat after phases with and without sediment input. The stratigraphy is compiled from the measured bathymetry.

Table 1 Summary of flume tank experiments with variable slope angles and current velocities (experiments 2-6).

Experiment	Figure	Slope angle [°]	Velocity [cm/s]	Moat width [cm]	Moat relief [cm]	Moat aspect ratio	Drift angle [°]
2	4a	18	11	-	-	-	-
3	4b	18	16	28.5	1	0.04	8
4	4c	18	18	42.5	3.8	0.09	11
5	4d	26	11	44.0	1.1	0.02	4
6	4e	26	16	47.0	3.6	0.08	15

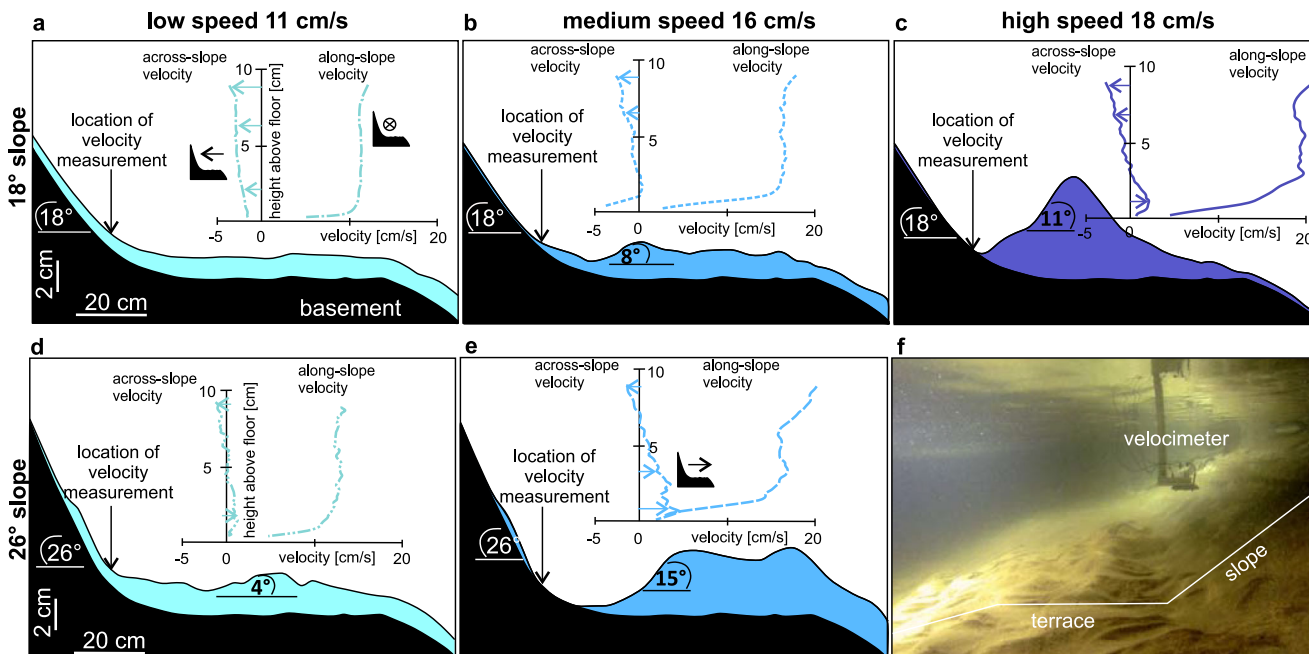


Fig. 4 Comparison of moat-drift systems developed at a gentle and a steep slope with different velocities shows that steep slopes and faster currents lead to a steep drift (Experiment 2-6). (a) Measured cross-sections showing aggradation. (b-e) Measured cross-sections from moat-drift systems show that the morphology depends on current speed and slope gradient. The graph shows the along-slope and across-slope velocity measured at the lower slope at the beginning of the experiment (basement morphology, before the sediment deposition and moat-drift system formation). Positive across-slope velocities correspond to a current flowing away from the slope. (f) Underwater photo of the moat-drift system in the flume tank that developed at a current speed of 18 cm/s and a slope angle of 18°.

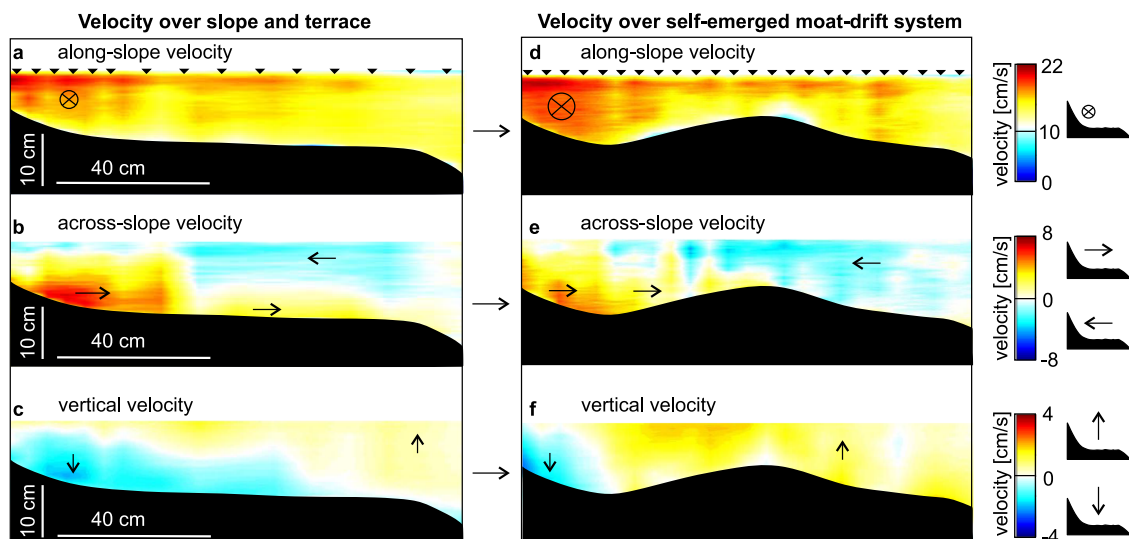


Fig. 5 Velocity across-slope obtained with the fastest current setting. Velocity measurements at the beginning of the experiments in (a) along-slope direction; (b) across-slope direction; (c) vertical direction. Velocity measurements after moat-drift system emerged in (d) along-slope direction; (e) across-slope direction; (f) vertical direction. Note: the color scale varies between the plots. The velocimeter location is indicated by black triangles. The location of the cross-sections is shown in Fig. 2.

upwards (Fig. 5c). After the moat-drift system self-emerged, the velocity is measured again (Fig. 5d, e). The velocity increased over the area above the moat compared to the measurements before the moat formed. The velocity is higher over the moat and decreases over the drift (Fig. 5d). The across-slope velocity near the seafloor between the slope and drift crest is directed away from the slope, but between drift crest and basin, it is directed toward the slope (Fig. 5e). On the slope, the velocity is directed downwards, and everywhere else it is directed upwards (Fig. 5f).

Discussion

Comparison between experiments and natural systems. An open question in the study of marine natural systems is that the flow conditions that initially started to create a specific morphology, like a contourite drift, remain unknown because there are no oceanographic measurements from when the features started to form. Moreover, these sedimentary features take thousands to millions of years to form. To overcome this issue, we created a simple setup in a flume tank in which moat-drift systems can form, to allow us to investigate their evolution over time. The setup of the experiment consists of an upper slope and a terrace representing a continental margin that is, for example, analogous to the Argentine continental margin²⁵. However, the experiments are not limited to this setting and also represent other settings in which the slope gradient changes. In natural systems, moats commonly form when there is a break in the slope gradient^{4,17}. This is for example the case at the edge of the slope at the Great Bahamas Bank, the Cay Sal Bank²⁶, at the foot of a topographic obstacle offshore Galicia²⁷, offshore Mozambique (Beira Moat)²⁸, offshore north Spain (Gijón Moat)²⁹ or commonly around cold-water coral mounds¹. For the experiments, we chose a slope angle of 18° and 26°, which is steeper than the average slopes of continental margins, which are often below 10°³⁰. However, local steeper slopes are common in many environments, they can exist for instance around topographic obstacles, ridges or seamounts^{27,31}. Measurements from 38 different locations worldwide show that typical values for moat-drift systems are a 50 m relief (between 4 m and 505 m), 2.3 km width (between 200 m and up to 35 km), 0.022 relief-width ratio (between 0.003 and 0.1), 6° slope angle (between 0.3° and 25°) and 3° drift angle (between 0.5° and 17°)^{17,32}. The experiment in

the flume tank thus represents a situation with particularly high slopes. These do not represent the average continental slope, but are realistic dimensions. Slopes on which the moats form are often especially high around seamounts or other topographic obstacles. For example the Galicia Moat, located at a topographic obstacle is located at an 25° slope^{17,27}. Since these topographic obstacles are not always covered by sediment and can thus not be eroded by the current, the slope angle must have been the same when the moat-drift system formed. Similar to the deep sea, the drift angle of the moats in the flume tank (4°–15°) is lower than the slope angle. The moats in the flume tank have a similar aspect ratio (0.02–0.9) compared to moats in nature (see Supplementary Note 3).

The experiments demonstrate that the development of a contourite depositional system depends on sediment input. When sediment is added to the 18 cm/s strong contour current, the moat-drift system migrates upslope, similar to some moat-drift systems in deep-marine environments^{6,10,19,29,31}. In the deep sea, moat-drift systems can also migrate downslope^{33,34}. In the experiments, the deposits differ between a current transporting sediments and the same current not transporting sediments. Sediment is deposited if the sediment transport capacity is exceeded. When a current of similar strength has a relatively low sediment load, it may pick up sediment until its transport capacity is reached. As a result, the moat-drift system can migrate downslope by reworking the side of the drift at the moat under constant contour current speed when no sediment is added to the contour current. Due to the erosion, the moat becomes wider and the relief increases. Thus, the migration direction depends on both current speed and sediment supply. A current with no sediments can erode, while the same current with more sediments than its transport capacity will deposit sediment. If the current speed for the moat-drift system is known, this can be used to understand sediment availability and how it has changed over time.

The internal stratigraphic architecture of the drift partly preserves the evolution of the morphological elements. The stacking pattern of the moat-drift systems that self-emerged in the flume tank is comparable to the recorded seismic reflection profiles from the deep sea. Erosional periods are identified by truncated reflections and depositional periods show sigmoidal

reflections. Our results indicate that the sediment supply during the experiment is high when the constructional moat-drift systems form. The constructional moat-drift system in the flume tank (Fig. 3c) is comparable to the downstream cross-section of the Álvarez Capral Moat in the Gulf of Cadiz (Fig. 1b). The erosional moat-drift system (Fig. 3d) shows truncations at the drift side, which are similar to an upstream cross-section from the Álvarez Capral Moat (Fig. 1a). In this part of the system, the current must be intense and/or the sediment supply must be low. Erosional and depositional periods can vary over time because ocean current speed and sediment supply change. In our experiments, variations in sediment supply under constant current-forcing led to a mixed constructional-erosional moat-drift system (Fig. 3e) similar to the Ewing Terrace Moat 2 at the northern Argentine margin¹⁵.

Current dynamics and sediment transport pathways over the slope and terrace. The hydrodynamics of the current when the moat-drift system initially started to form is so far unknown. Our experiments show that the current is flowing primarily parallel to the slope. The current speed is higher near the slope and decreases over the terrace, already before the formation of a moat-drift system. This is due to the circular current that has a higher speed away from the vortex center and becomes zero in the center of the vortex. Furthermore, the depth decreases above the slope and thus the centrifugated and thinned water mass needs to increase its velocity in order to preserve centrifugal vorticity. Thus, the centripetal pressure gradient depends on the slope angle and current speed (see Supplementary Note 1).

The velocity measurements in the flume tank show that a secondary basinward flow can occur before the moat-drift system is established (Fig. 5a). Because of the rotating current there is a superelevated surface and an inward directed pressure gradient (see Supplementary Note 1). The centripetal force required for radial acceleration is caused by this inward directed pressure gradient. This centripetal pressure gradient is barotropic (constant in depth), but the velocity decreases towards the bed due to bed friction. Because of this, the slow-moving particles near the bed are accelerated away from the slope (inwards of the tank), while the fast flowing particles higher up in the water column are flowing toward the slope (outwards), resulting in a secondary flow near the bottom. Conservation of volume is achieved by the downward and upward water exchanges between the lateral flows, which leads to a helix flow over the moat. This current is recorded by the across-slope velocity measurements and shows that the secondary flow directed downslope and across the terrace at the lowest ~5 cm above the seafloor. Furthermore, when the current velocity is increased, both centrifugal and centripetal force become higher and the secondary flow increases (Fig. 4c). Similarly in nature, the bottom boundary Ekman transport also increases with higher current velocity³⁵. Cross-shelf Ekman transport can occur in a rotating frame in the frictional boundary layer when a current flows over a sloping seabed³⁶. It can transport dense water upslope or light water downslope, depending on the hemisphere and current direction^{35–39}. When the slope gradient is increased, also the horizontal pressure gradient increases, thereby enhancing the secondary flow⁴⁰. As a result, a steeper slope and a faster current lead to a stronger secondary flow. When the secondary flow becomes stronger, more sediment may be transported from the slope towards the drift.

In all experiments where a secondary flow is recorded, a moat-drift system later self-emerges. If no secondary flow is recorded, only aggradation occurs on the terrace and no moat-drift system is established. This situation occurred at the combination of the

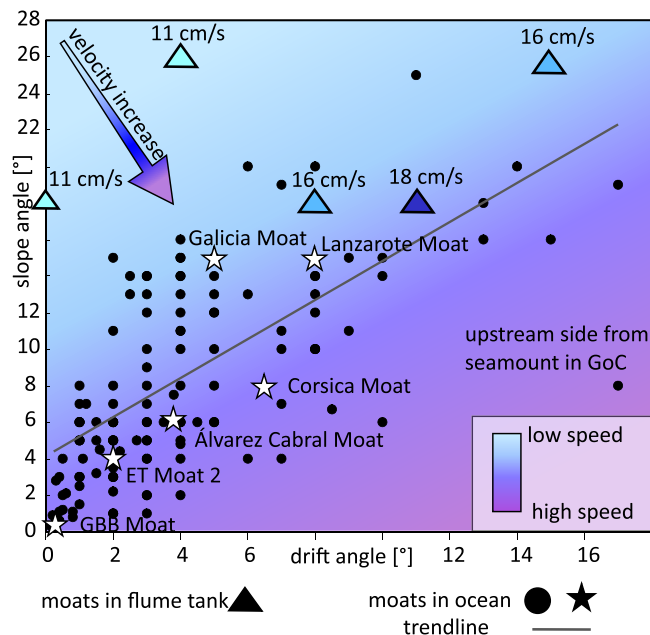


Fig. 6 Diagram showing the link between current speed, slope angle and drift angle. Moats in the ocean are obtained from^{17,32}. Abbreviations: GoC: Gulf of Cadiz, ET Moat 2: Ewing Terrace Moat 2 offshore Argentina, GBB Moat: Great Bahamas Bank Moat in the Bahamas.

lowest velocity and lowest slope in our experiments (Fig. 4a). In natural systems, this occurs for example at the La Plata terrace at the Argentine margin south of the Mar del Plata canyon⁴¹. In summary, we suggest that a current with a velocity that is strong enough to transport particles together with a secondary flow near the seabed is necessary for a moat-drift system to develop. This means that there is a threshold below which no moat-drift system can form, which agrees with observations³² from many locations at continental margins where no moat-drift systems form (Fig. 6).

Some authors suggest that the moat formation, or contourite formation in general, could be also influenced by internal waves or turbulence at the density contrast between two water masses^{4,20,22,27,42–44}. Others suggest that they form in association with ocean current surface fronts^{27,45}. Our experiments show that moat-drift systems can form solely with along-slope currents if sediment is available to be transported and shaped into a drift deposit, without any of these additional oceanographic processes. However, the experiments do not disprove possible contributions of these other processes in natural systems because the processes were not tested in the experiments.

Current dynamics and sediment transport pathways of moat-drift systems. Moats are hypothesized to be related to the highly energetic cores of the current^{15,28,46–48}. Previous velocity measurements show an intensification in bottom current velocity over a moat and lower speeds over the drift and terrace offshore north Argentina (Fig. 1c)¹⁵. This is also observed during the velocity measurements over the moat-drift system in the flume tank. It was speculated that the current velocity is increased over the moat due to the morphology of the moat, which could stabilize and focus the bottom current by limiting the variability in the cross-slope direction¹⁵. This hypothesis is supported by the flume tank experiments.

Several authors hypothesized that there is a secondary flow with a helicoidal structure over moats, but the suggested direction differs between authors, and this interpretation has not been supported by measurements yet^{4,21,24}. The velocity

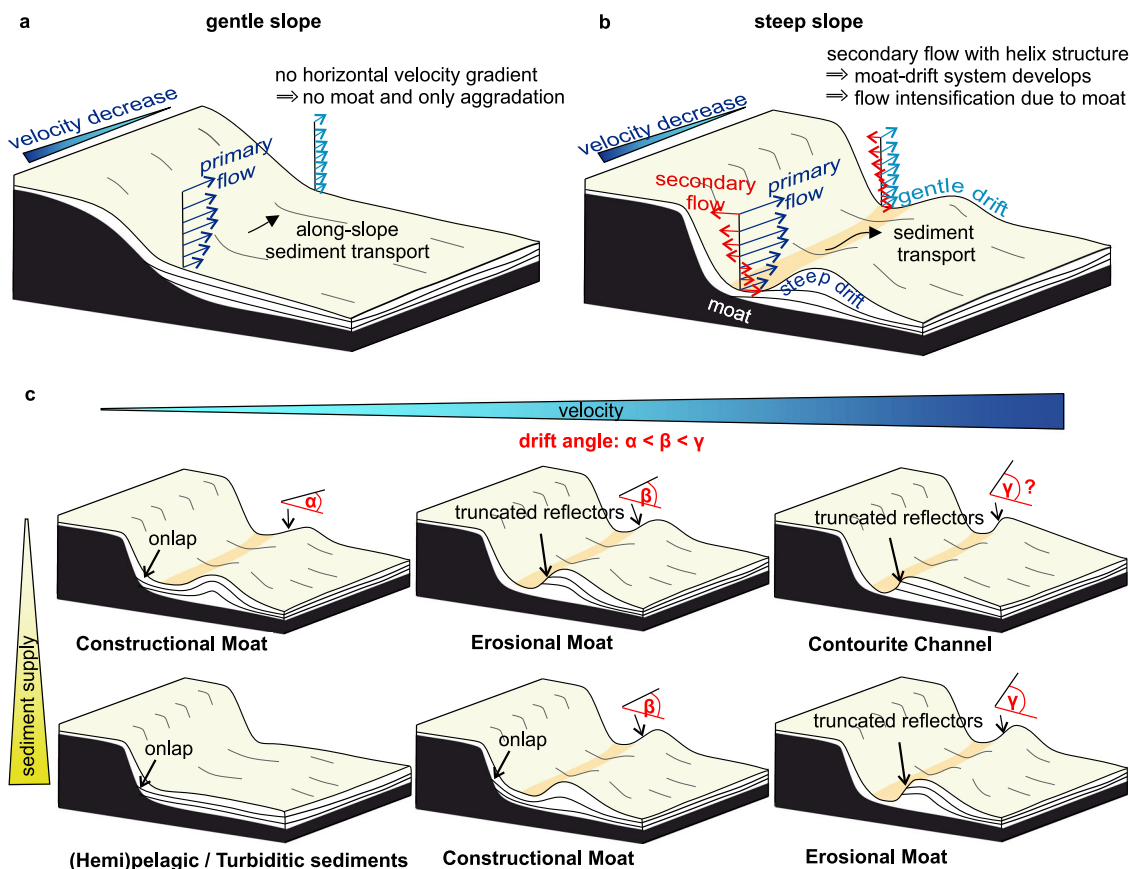


Fig. 7 Conceptual model of current and sediment dynamics over the moat-drift system. (a) At a gentle slope with a low current speed only aggradation occurs. (b) The moat-drift system forms if there is a secondary flow near the seafloor that transports sediment from the slope toward the drift. In three dimensions, the current has a helicoidal structure and is confined inside the moat. The secondary flow decreases with lower speeds and more gentle slopes. The current speed and the slope's steepness influence the drift's steepness. (c) The type of moat, meaning if it is more depositional or erosional, depends on the sediment supply and the current speed. α , β , γ represent the drift angle.

measurements carried out during the experiments show, for the first time, the previously suspected secondary flow with a helix-structure within the moat (Fig. 5e, f). The orientation of the helix within the moat remains stable upon moat formation: the near-bottom flow is always directed offshore, and the top of the helix is always directed towards the slope. This observed spinning direction of the helix flow within the moat is in agreement with the previously hypothesized helix flow of some authors⁴. In our experiments, the secondary circulation is contained within the moat by the drift, and it does not continue flowing over the terrace (Fig. 5e). This enclosure of the helix within the moat coincides with an increase of the primary along-slope velocity component, which suggests that moat-drift formation provides a fundamental mechanism for contour-current strength enhancement.

Current speed reconstructions based on morphology. The experiments show that steeper slopes and faster currents lead to steeper drifts next to a moat (Figs. 4 and 6). The experiments that only lead to aggradation on the terrace when the velocity and/or the slope angle are too low for moat-drift formation (Fig. 4) indicate that for a specific current speed, a minimum slope angle exists to allow moat-drift system formation.

Plotting the slope angle against the drift angle shows that data points clustering in the upper left corner (meaning high slope and low drift angle) are related to low current speeds. The experimental data exhibit a trend whereby the lowest velocities plot to the top left of the diagram (steep slope and low drift angle),

and the faster velocities to the bottom right (lower slope and higher drift angle; Fig. 6). This trend is also observed for moat-drift systems in the deep sea, but the trend is unclear due to the limited amount of data and the short velocity recording period. For example, velocity data shows an average bottom current speed over the Great Bahamas Bank Moat of 36 cm/s and for the Ewing Terrace Moat 2 offshore north Argentina of 29 cm/s^{15,26}. We use this structure to suggest interpretations of natural conditions from slope-moat-drift architectures. For example, the Galicia Moat²⁷ and Lanzarote Moat⁴⁹ have the same slope angle but different drift angles. Our results suggest that the drift angle from Lanzarote Moat is higher because the current speed is higher. Our results also suggest that Ewing Terrace Moat 2¹⁵, Alvarez Cabral Moat⁵⁰, and Corsica Moat³¹ are probably formed under similar current speeds and the difference in drift angle is likely due to differences in the slope angle.

Results from topographic obstacles seem to be less reliable for the current reconstruction because such environments are often strongly diverted from the trendline, e.g., at the upstream side of topographic obstacles in the Gulf of Cadiz (Fig. 6). This might be linked to a less constant current along the slope of seamounts that could be related to changes in the direction in which the current hits the slope of the seamount. Whether these systems mainly react to mean or peak velocity remains unknown. Numerically modeled bottom currents over moats show high variability in current speed in the Mozambique channel and at the north-west Spanish margin, which suggests that moats and drifts are not necessarily continuously formed but rather more episodic^{10,20}.

Future flume tank experiments can test the influence of velocity variability. The present results from the flume tank experiments are limited to one range of sediment grain size. Thus, future experiments can test the influence of different sediment compositions and grain sizes on contourite development.

Conclusions

This study presents to the best of our knowledge the first experiments in which a contourite depositional system self-emerges in a three-dimensional flume tank, with no prior formation of any contourite feature. The experiments demonstrate the hydrodynamic and morphologic conditions necessary to form moat-drift systems. Taking into account the influence of current speed, slope and drift angle, together with the secondary flow measured in the flume tank, we suggest (Fig. 7):

1. The moat-drift system is only able to form if there is a secondary flow near the seafloor that transports sediment from the slope toward the drift (basinward). The secondary flow increases with higher speeds and steeper slopes.
2. After the moat is formed, the secondary flow is confined in the moat and has a helicoidal flow structure. The along-slope velocity becomes more focused and increases.
3. Migration of the moat, and formation of internal stratigraphic architecture, is a function of current strength in combination with sediment availability. Low sediment availability leads to migration towards the terrace, and truncation of reflectors. High sediment availability leads to migration towards the slope and formation of sigmoidal deposits on the terrace-side of the moat.
4. Higher current speeds and steeper slopes lead to a steeper sediment drift. Thus, current speed reconstructions from seismic data or bathymetric data are possible but the slope angle must be taken into account when the current speed is reconstructed. This shows that moat-drift systems can be used for paleo-velocity estimates, which allows reconstructions of current speed and direction over the past millions of years. This might be an important step forward for paleocurrent reconstructions.

Materials and methods

The experiments are conducted in a 6 m wide, 11 m long, and 1 m deep flume tank. The floor morphology consists of a gentle lower slope (not part of the study area), a flat terrace, and an upper slope of 18° or 26°. The morphology is built out of sediment and then covered by artificial grass (grass made out of plastic). The artificial grass stabilizes the morphology that forms the base of each experiment. The artificial grass is covered before the first experiments by a thin 1.5 cm layer of walnut shells and for experiments 2–6 by a 0.5 cm thick layer. Based on this starting morphology, we conduct different experiments. We removed all added walnut shells after each experiment.

During the experiments, 3 pumps created a current flowing clockwise in the tank and parallel to the slope at the study area, which is an analog to a contour current flowing parallel to a continental margin (similar to⁵¹). Since the Earth rotates, ocean currents are affected by the Coriolis force. In the lab, the size of the experiment is too small for the Coriolis force to have a notable effect. For gravity-driven currents a rotating flume tank has been used in previous studies^{52,53}. For contour currents, we use a current flowing in a circular motion. Run-up against the slope provides a barotropic pressure gradient that forces the radial acceleration of the circulation. We consider this as a simplified analog to the Coriolis effect in a natural system (see Supplementary Note 1). An UDOP 4000 velocimeter measures the

velocity during the experiments. One 1 MHz probe is the emitter, and three probes are used as receivers to record the velocity in 3D. The UDOP was positioned ~15 cm above the bed at the beginning of the experiment. In the first 5 cm near the emitter, the data quality is poor, and the data is not usable. The velocity measurements shown in Fig. 4 were carried out within the first 20 min of the experiments, which is before the moat-drift system was established. For the across-slope profile, the velocity was measured every 5–10 cm for 2 min. When the velocity was not measured, the instrument was positioned in the middle of the tank to ensure that it does not influence the current- and morpho-dynamics of the study area.

In the experiments, two phases are distinguished. One is the sediment input phase where sediment is added and the other is the sediment reworking phase where no sediment is added. In the first experiment, the first sediment input phase is 3 h, the reworking phase is 8 h and the second input phase is 7 h. In experiments 2–6, the sediment input phase is 3 h, and the reworking phase is 4 h. During the beginning of the sediment input phase, a pump on the side of the flume tank pumped water mixed with 80 dm³ of crushed walnut shells of a volume concentration below 2% for 2 h into the flume tank. This is similar to sediment entering the ocean by rivers, turbidity currents or marine production, which are then transported by along-slope currents⁵⁴. The particles are transported to the study site by the contour current and start to settle there. The contour current reworks the previously deposited walnut shells. Contourite drifts are often composed of fine-grained sediments^{4,10}. In previous studies walnut shells were used as an analog for mud in estuaries⁵⁵. The experiments were conducted with crushed walnut shells with a grain size range of 200–450 µm and a density of 1350 kg/m³. According to Stokes' law, these walnut shells settle with a velocity of 1.9 cm/s. The calculated flow shear velocity for the used 11 cm/s, 16 cm/s and 18 cm/s current is 1.1 cm/s, 1.6 cm/s and 1.8 cm/s, respectively (see Supplementary Note 2). We use walnut shells as an analog for silt because similar current speeds transport the particles as bedload. The advantage of the coarse walnut shell over the fine silt is that the settling velocity is higher due to the larger diameter, which allows us to run the experiments in a smaller setup. The crushed walnut shells are then transported as bedload similar to silt because they are coarser but have a lower density. The non-dimensional bed shear stress (Shields parameter) is 0.11, 0.22 and 0.28 for the used 11 cm/s, 16 cm/s and 18 cm/s current speeds. These values exceed the critical threshold of 0.05, meaning sediment is transported.

Before the experiment, and after the experiment, once the tank is drained, a laser scanner measures the bathymetry in the flume tank, every 2 mm with a swath width of 50 cm on pre-defined across-slope profiles. The data result in a bathymetric map with a grid cell size of 5 mm.

Data availability

All data needed to evaluate the conclusions in the paper are present in the paper and are available on PANGAEA (<https://doi.org/10.1594/PANGAEA.956303>). Supplementary material for this article is available on YouTube (<https://youtu.be/J8NhFoTcUQg>).

Received: 23 January 2023; Accepted: 25 August 2023;

Published online: 06 September 2023

References

1. Hebbeln, D., Van Rooij, D. & Wienberg, C. Good neighbours shaped by vigorous currents: cold-water coral mounds and contourites in the North Atlantic. *Mar. Geol.* **378**, 171–185 (2016).

2. Kane, I. A. et al. Seafloor microplastic hotspots controlled by deep-sea circulation. *Science* **368**, 1140–1145 (2020).
3. Voosen, P. Climate change spurs global speedup of ocean currents. *Science* **367**, 612–613 (2020).
4. Rebesco, M., Hernández-Molina, F. J., Van Rooij, D. & Wåhlin, A. Contourites and associated sediments controlled by deep-water circulation processes: state-of-the-art and future considerations. *Mar. Geol.* **352**, 111–154 (2014).
5. Hernández-Molina, F. J. et al. Onset of mediterranean outflow into the North Atlantic. *Science* **344**, 1244–1250 (2014).
6. Uenzelmann-Neben, G., Weber, T., Grütznér, J. & Thomas, M. Transition from the cretaceous ocean to cenozoic circulation in the western South Atlantic—A twofold reconstruction. *Tectonophysics* **716**, 225–240 (2017).
7. McCartney, M. S. The subtropical recirculation of mode waters. *J. Mar. Res.* **40**, 64 (1982).
8. McCave, I., Manighetti, B. & Robinson, S. Sortable silt and fine sediment size/composition slicing: parameters for palaeocurrent speed and palaeoceanography. *Paleoceanography* **10**, 593–610 (1995).
9. McCave, I. N. Formation of sediment waves by turbidity currents and geostrophic flows: a discussion. *Mari. Geol.* **390**, 89–93 (2017).
10. Miramontes, E. et al. Contourite and mixed turbidite-contourite systems in the mozambique channel (SW Indian Ocean): link between geometry, sediment characteristics and modelled bottom currents. *Mar. Geol.* **437**, 106502 (2021).
11. Wu, S. et al. Orbital-and millennial-scale Antarctic circumpolar current variability in drake passage over the past 140,000 years. *Nat. Commun.* **12**, 1–9 (2021).
12. Stow, D. A. et al. Bedform-velocity matrix: the estimation of bottom current velocity from bedform observations. *Geology* **37**, 327–330 (2009).
13. Stow, D. & Smillie, Z. Distinguishing between deep-water sediment facies: turbidites, contourites and hemipelagites. *Geosciences* **10**, 68 (2020).
14. de Lavergne, C., Madec, G., Capet, X., Maze, G., & Roquet, F. Getting to the bottom of the ocean. *Nat. Geosci.* **9**, 857–858 (2016).
15. Wilckens, H. et al. The erosive power of the malvinas current: influence of bottom currents on morpho-sedimentary features along the northern Argentine margin (SW Atlantic Ocean). *Mar. Geol.* **439**, 106539 (2021).
16. Frey, D. et al. Direct measurements of the malvinas current velocity structure. *J. Geophys. Res.: Oceans* **126**, e2020J0016727 (2021).
17. Wilckens, H. et al. Factors controlling the morphology and internal sediment architecture of moats and their associated contourite drifts. *Sedimentology* **70**, 1472–1495 (2023).
18. Surlyk, F. & Lykke-Andersen, H. Contourite drifts, moats and channels in the upper cretaceous chalk of the danish basin. *Sedimentology* **54**, 405–422 (2007).
19. Betzler, C., Lüdmann, T., Hübscher, C. & Fürstenau, J. Current and sea-level signals in periplatform ooze (Neogene, Maldives, Indian Ocean). *Sediment. Geol.* **290**, 126–137 (2013).
20. Zhang, W., Hanebuth, T. J. & Stöber, U. Short-term sediment dynamics on a meso-scale contourite drift (off NW Iberia): Impacts of multi-scale oceanographic processes deduced from the analysis of mooring data and numerical modelling. *Mar. Geol.* **378**, 81–100 (2016).
21. Hernández-Molina, F., Llave, E. & Stow, D. Continental slope contourites. *Dev. Sedimentol.* **60**, 379–408 (2008).
22. Miramontes, E. et al. The impact of internal waves on upper continental slopes: insights from the Mozambican margin (southwest Indian Ocean). *Earth Surf. Processes Landf.* **45**, 1469–1482 (2020).
23. Tucholke, B. E. & Ewing, J. I. Bathymetry and sediment geometry of the greater Antilles outer ridge and vicinity. *Geol. Soc. Am. Bull.* **85**, 1789–1802 (1974).
24. Gong, C., Peakall, J., Wang, Y., Wells, M. G. & Xu, J. Flow processes and sedimentation in contourite channels on the northwestern South China Sea margin: a joint 3D seismic and oceanographic perspective. *Mar. Geol.* **393**, 176–193 (2017).
25. Hernández-Molina, F. J. et al. Contourite depositional system on the Argentine Slope: an exceptional record of the influence of Antarctic water masses. *Geology* **37**, 507–510 (2009).
26. Lüdmann, T. et al. Carbonate mounds in the santaren channel, bahamas: a current-dominated periplatform depositional regime. *Mar. Geol.* **376**, 69–85 (2016).
27. Hanebuth, T. J., Zhang, W., Hofmann, A. L., Löwemark, L. A. & Schwenk, T. Oceanic density fronts steering bottom-current induced sedimentation deduced from a 50 ka contourite-drift record and numerical modeling (off NW Spain). *Quat. Sci. Rev.* **112**, 207–225 (2015).
28. Thiéblemont, A., Hernández-Molina, F. J., Miramontes, E., Raison, F. & Penven, P. Contourite depositional systems along the Mozambique channel: the interplay between bottom currents and sedimentary processes. *Deep Sea Res. Part I: Oceanogr. Res. Pap.* **147**, 79–99 (2019).
29. Liu, S., Hernández-Molina, F. J., Ercilla, G., & Van Rooij, D. Sedimentary evolution of the Le Danois contourite drift systems (southern Bay of Biscay, NE Atlantic): a reconstruction of the Atlantic Mediterranean Water circulation since the Pliocene. *Mar. Geol.* **427**, 106217 (2020).
30. O’Grady, D. B., Syvitski, J. P., Pratson, L. F. & Sarg, J. Categorizing the morphological variability of siliciclastic passive continental margins. *Geology* **28**, 207–210 (2000).
31. Miramontes, E. et al. The Pianosa contourite depositional system (northern Tyrrhenian Sea): drift morphology and Plio-Quaternary stratigraphic evolution. *Mar. Geol.* **378**, 20–42 (2016).
32. Wilckens, H. et al. Morphological properties of moat-drift systems around the world. *PANGAEA* <https://doi.org/10.1594/PANGAEA.955053> (2023).
33. Hernández-Molina, F. J. et al. Oceanographic processes and morphosedimentary products along the Iberian margins: a new multidisciplinary approach. *Mar. Geol.* **378**, 127–156 (2016).
34. Rebesco, M. et al. Evolution of a high-latitude sediment drift inside a glacially-carved trough based on high-resolution seismic stratigraphy (Kveithola, NW Barents Sea). *Quat. Sci. Rev.* **147**, 178–193 (2016).
35. Wåhlin, A. et al. Some implications of ekman layer dynamics for cross-shelf exchange in the Amundsen Sea. *J. Phys. Oceanogr.* **42**, 1461–1474 (2012).
36. Ekman, V. W. On the influence of the Earth’s rotation on ocean- currents. *Ark. Mat. Astron. Fys.* **2**, 1–52 (1905).
37. Trowbridge, J. & Lentz, S. Asymmetric behavior of an oceanic boundary layer above a sloping bottom. *J. Phys. Oceanogr.* **21**, 1171–1185 (1991).
38. Weatherly, G. L. A numerical study of time-dependent turbulent Ekman layers over horizontal and sloping bottoms. *J. Phys. Oceanogr.* **5**, 288–299 (1975).
39. Weatherly, G. L. & Martin, P. J. On the structure and dynamics of the oceanic bottom boundary layer. *J. Phys. Oceanogr.* **8**, 557–570 (1978).
40. Salon, S., Crise, A., & Van Loon, A. Dynamics of the bottom boundary layer. *Dev. Sedimentol.* **60**, 83–97 (2008).
41. Preu, B. et al. Sedimentary growth pattern on the northern Argentine slope: the impact of North Atlantic Deep Water on southern hemisphere slope architecture. *Mar. Geol.* **329–331**, 113–125 (2012).
42. Preu, B. et al. Morphosedimentary and hydrographic features of the northern Argentine margin: the interplay between erosive, depositional and gravitational processes and its conceptual implications. *Deep Sea Res. Part I: Oceanogr. Res. Pap.* **75**, 157–174 (2013).
43. Hernández-Molina, F. J. et al. A contourite depositional system along the Uruguayan continental margin: sedimentary, oceanographic and paleoceanographic implications. *Mar. Geol.* **378**, 333–349 (2016).
44. Shanmugam, G. Modern internal waves and internal tides along oceanic pycnoclines: challenges and implications for ancient deep-marine baroclinic sands. *Internal waves, internal tides, and baroclinic sands. AAPG Bull.* **97**, 799–843 (2013).
45. Nicholson, U. & Stow, D. Erosion and deposition beneath the subantarctic front since the early oligocene. *Sci. Rep.* **9**, 1–9 (2019).
46. Yin, S. et al. The influence of oceanographic processes on contourite features: a multidisciplinary study of the northern South China Sea. *Mar. Geol.* **415**, 105967 (2019).
47. Llave, E. et al. Contourites along the Iberian continental margins: conceptual and economic implications. *Geol. Soc. Lond. Spec. Publ.* **476**, 403–436 (2020).
48. De Castro, S. et al. Contourite characterization and its discrimination from other deep-water deposits in the Gulf of Cadiz contourite depositional system. *Sedimentology* **68**, 987–1027 (2021).
49. Acosta, J. et al. in *Geophysics of the Canary Islands* 41–57 (Springer, 2005).
50. Garcia, M. et al. Contourite erosive features caused by the mediterranean outflow water in the Gulf of Cadiz: quaternary tectonic and oceanographic implications. *Mar. Geol.* **257**, 24–40 (2009).
51. Miramontes, E. et al. Channel-levee evolution in combined contour current–turbidity current flows from flume-tank experiments. *Geology* **48**, 353–357 (2020).
52. Wells, M. & Cossu, R. The possible role of Coriolis forces in structuring large-scale sinuous patterns of submarine channel–levee systems. *Philos. Trans. R. Soc. A: Math. Phys. Eng. Sci.* **371**, 20120366 (2013).
53. Lentz, S. J. & Helfrich, K. R. Buoyant gravity currents along a sloping bottom in a rotating fluid. *J. Fluid Mech.* **464**, 251–278 (2002).
54. Razik, S., Govin, A., Chiessi, C. M. & von Döbenek, T. Depositional provinces, dispersal, and origin of terrigenous sediments along the SE South American continental margin. *Mar. Geol.* **363**, 261–272 (2015).
55. Ganti, V., Chadwick, A. J., Hassenruck-Gudipati, H. J., Fuller, B. M. & Lamb, M. P. Experimental river delta size set by multiple floods and backwater hydrodynamics. *Sci. Adv.* **2**, e1501768 (2016).

Acknowledgements

We thank Han de Witte for technical support with the experiments. This work has been done in collaboration within the “The Drifters” Research Group at Royal Holloway University of London (RHUL). We thank TGS for their permission to use the seismic profile of the Álvarez Cabral Moat in Fig. 1. H.W.’s research stay at the Utrecht University was supported by the BremenIDEA funding line from the University of Bremen. We thank the reviewers Kyle Strom, George Pantopoulos and Chenglin Gong, and

Primary Editor Joe Aslin for their constructive comments that greatly improved our manuscript.

Author contributions

H.W. and E.M. conceived the study. J.T.E., H.W., E.M. and P.H.A. designed the experiments. H.W. performed the experiments and visualized the data. E.M., J.T.E. supervised the study. H.W., E.M., J.T.E., P.H.A., F.J.H.M. and R.S.J. discussed the data interpretation. H.W. wrote the original draft and all authors edited it.

Funding

Open Access funding enabled and organized by Projekt DEAL.

Competing interests

The authors declare no competing interests.

Additional information

Supplementary information The online version contains supplementary material available at <https://doi.org/10.1038/s43247-023-00978-0>.

Correspondence and requests for materials should be addressed to Henriette Wilckens.

Peer review information *Communications Earth & Environment* thanks Kyle Strom,

George Pantopoulos and Chenglin Gong for their contribution to the peer review of this work. Primary Handling Editor: Joe Aslin.

Reprints and permission information is available at <http://www.nature.com/reprints>

Publisher's note Springer Nature remains neutral with regard to jurisdictional claims in published maps and institutional affiliations.



Open Access This article is licensed under a Creative Commons Attribution 4.0 International License, which permits use, sharing, adaptation, distribution and reproduction in any medium or format, as long as you give appropriate credit to the original author(s) and the source, provide a link to the Creative Commons licence, and indicate if changes were made. The images or other third party material in this article are included in the article's Creative Commons licence, unless indicated otherwise in a credit line to the material. If material is not included in the article's Creative Commons licence and your intended use is not permitted by statutory regulation or exceeds the permitted use, you will need to obtain permission directly from the copyright holder. To view a copy of this licence, visit <http://creativecommons.org/licenses/by/4.0/>.

© The Author(s) 2023